Imaging biomarkers for primary motor outcome after stroke – should we include information from beyond the primary motor system?

Christoph Sperber, PhD, Johannes Rennig, PhD, Hans-Otto Karnath, MD, PhD

Centre of Neurology, Division of Neuropsychology, Hertie-Institute for Clinical Brain Research, University of Tübingen, Tübingen

Corresponding Author:
Christoph Sperber
Centre of Neurology
University of Tübingen
72076 Tübingen
Germany
e-mail: christoph.sperber@klinikum.uni-tuebingen.de

Abstract

Hemiparesis is a common consequence of stroke to the primary motor system. Previous studies suggested that damage to additional brain areas might play a causal role in occurrence and severity of hemiparesis and its recovery. Imaging biomarkers to predict post stroke outcome thus might also account for damage to these non-primary motor areas. The study aimed to evaluate if damage to areas outside of the primary motor system is predictive of hemiparesis, and if this damage plays a causal role in its occurrence. In 102 patients with unilateral stroke, the neural correlates of acute and chronic upper limb paresis were mapped by univariate and multivariate lesion behaviour mapping. Following the same approach, CST lesion biomarkers were mapped, and resulting topographies of both analyses were compared. All mapping analyses of acute or chronic upper limb paresis implicated areas outside of the primary motor system. Likewise, mapping CST lesion biomarkers – that, by definition, are only causally related to damage of the CST – implicated several areas outside of the CST with high correspondence to areas associated with upper limb paresis. Damage to areas outside of the primary motor system might not play a causal role in hemiparesis, while still providing predictive value. This finding suggests that simple theory-based biomarkers or qualitative rules to infer post-stroke outcome from imaging data might perform sub-optimally, as they do not consider the complexity of lesion data. Instead, high-dimensional models with data-driven feature selection strategies might be required.

Introduction

Brain lesions through strokes are a leading cause of acquired disability, and motor deficits such as weakness or paresis of the limbs are among its most common and debilitating symptoms. Such deficits arise after damage to the primary motor system, i.e. the primary motor cortex and its projection fibre, the corticospinal tract (CST). It is widely assumed that damage of the corticospinal tract underlies persisting primary motor deficits (Lindenberg et al., 2010; Lo et al., 2010; Zhu et al., 2010; Park et al., 2016). Thus, strategies to predict long-term motor outcome focused on assessing CST integrity by brain imaging (Lindenberg et al., 2010; Stinear et al., 2012; Wang et al., 2012; Sterr et al., 2014; Buch et al., 2016) or neurostimulation (Stinear et al., 2012).

Several studies developed prediction algorithms for motor outcome solely based on measures of CST damage derived from clinical CT or MR imaging (Wenzelburger et al., 2005; Zhu et al., 2010; Feng et al., 2015; Findlater et al., 2019). Metrics of CST lesion load were derived by referencing topographical lesion data to probabilistic topographies of the CST obtained by fibre tracking in healthy controls (Zhu et al., 2010; Feng et al., 2015; Findlater et al., 2019). These metrics were used in low-dimensional regression methods to predict motor outcome with moderate precision. However, two prediction studies using high-dimensional regression methods achieved better predictions if voxel-wise features were not only selected within the primary motor system, i.e. the CST and primary motor cortex, but, additionally, from a set of frontal, subcortical, and parietal areas (Rondina et al., 2016; Rondina et al., 2017). The authors hypothesized that integrity of these regions plays a role in both motor deficits and motor recovery for their relation to motor and sensory function according to the literature. In other words, they performed a theory-driven feature selection, which resulted in improved prediction performance. A similar study found that in patients with stroke not confined to subcortical areas, using features taken from outside the CST improves model quality (Park et al., 2016). These finding are complimentary to lesion-behaviour mapping studies that found neural correlates of hemiparesis outside primary motor regions. Disintegrity of a cingulo-opercular attention control network was found to contribute to motor deficits (Rinne et al., 2017). Association fibres, the insula, and perisilvian areas were found to be associated with primary motor deficits in right hemisphere stroke, underlining a possible role of right hemisphere brain networks in motor recovery (Frenkel-Teledo et al., 2019). Another study found putamen and several fibre tracts to be associated with poor

motor outcome (Findlater et al., 2019). Taken together, these findings suggest that stroke to regions outside the primary motor system might contribute to primary motor deficits. The identification of such regions thus is of high relevance in motor outcome prediction, as it provides a foundation for feature selection.

A possible objection against the relevance of non-primary motor regions comes from critical discussions on lesion-deficit inference. Topographical results in lesion behaviour mapping have been found to be biased by typical lesion anatomy (Mah et al., 2014; Sperber et al., 2019). It was postulated that the differentiation between areas where brain damage causes a deficit and areas where damage simply coincides with a deficit is impossible with current implementations of lesion-deficit inference (Sperber, 2020). Thus, strictly speaking, findings in previous studies might not be wrong, however, the causal interpretation of their role might be misattributed. On the other hand, information outside of brain regions where damage causes a symptom can bear predictive value for a symptom (Sperber, 2020). Hence, current feature selection strategies to choose imaging biomarkers in a theory-driven fashion might fall short, e.g. if motor outcome prediction is based only on information taken from regions where we assume damage to actually cause a long-lasting deficit.

The present study aimed to re-evaluate brain lesion-behaviour associations in upper limb paresis in 102 stroke patients. We used lesion behaviour mapping to identify regions associated with or holding predictive value for both acute and chronic upper limb paresis. We compared these topographies to regions associated with CST lesion biomarkers, which, per definition, are only causally related to damage to the CST. We hypothesized upper limb paresis to be associated with areas outside the primary motor system, either because damage in these areas actually contributes in some way to primary motor deficits, or because damage coincides with damage to the primary motor system. Further, we also hypothesized CST lesion biomarkers to be associated with regions outside the CST. Latter finding would hint at brain areas where damage does not play any causal role for hemiparesis, while it still bears predictive value.

Methods

Patient recruitment and motor assessment

Patients with a first unilateral cerebral stroke admitted to the Centre of Neurology at the University of Tübingen were recruited. Diagnosis was confirmed by CT or MRI

imaging. Patients with a medical history of other neurological or psychiatric disorders were excluded. All patients were re-examined in the chronic post-stroke stage at least 50 days and on average 423 days after the incident, and patients who suffered a second stroke were excluded. The final patient sample included 102 subjects (age = 59.9 years, SD = 13.0 years; 47 female, 55 male), of which 68 had stroke to the right, and 34 to the left hemisphere. The study has been performed in accordance with the standards laid down in the revised Declaration of Helsinki and patients or their relatives consented to the scientific use of the data.

Paresis of the upper limb was assessed by the BMRC (British Medical Research Council) scale on average 1.0 days (SD = 2.2 days) after stroke onset. The BMRC scoring ranges from zero to five (0: no movement, 1: palpable flicker, 2: movement without gravity, 3: movement against gravity 4: movement against resistance, 5: normal movement) and allows intermediate decimals in steps of 0.5. Ratings for distal and proximal upper limb motor function were averaged per patient.

Imaging and lesion delineation

Structural brain imaging was acquired by clinical CT or MRI on average 2.1 days (SD = 2.7 days) after stroke onset. If multiple scans were available, scans were chosen to be as acute as possible, while clearly depicting the borders of the lesion. If both suitable MRI and CT were available, MR scans were preferred. To visualize acute structural brain damage using MRI, diffusion weighted imaging was used in the first 48h after stroke onset, and T2 fluid attenuated inversion recovery imaging afterwards. If available, these images were co-registered with a high-resolution T1 MRI to be used in the normalization process.

Lesions were manually delineated on axial slices of the scans using MRIcron (https://www.nitrc.org/projects/mricron) by two experimenters, and the accuracy of lesion drawings was validated by consensus with the third experimenter. Scans were warped into 1x1x1 mm^3 MNI coordinates using age-specific templates in Clinical Toolbox (Rorden et al., 2012) and normalization algorithms in SPM 12 (www.fil.ion.ucl.ac.uk/spm), using cost-function masking to control for the lesioned area in the normalization process. The same normalization parameters were then applied to the lesion maps to obtain normalized binary lesion maps. Next, lesion maps of left hemisphere stroke patients were flipped along the sagittal mid-plane so that all lesions were depicted in the right hemisphere. This step was chosen as i) the study did

not aim to investigate possible hemisphere-specific contributions to primary motor skills, but general methodological aspects in mapping primary motor functions and recovery, and as ii) this ensured high statistical power and adequate sample sizes for multivariate lesion-behaviour mapping. Figure 1 shows a topography of all normalized lesion maps.

CST lesion biomarkers

We followed previous studies that computed CST lesion metrics to obtain biomarkers for post stroke motor outcome (Zhu et al. 2010; Feng et al., 2015; Findlater et al., 2019) and computed variables 'CST load' and 'weighted CST load'. Both metrics assess to what degree a structural lesion affects the CST by computing overlap metrics between a normalized lesion map and a probabilistic topography of the CST. The required probabilistic topography of the CST was taken from a publicly available white matter atlas based on diffusion tensor imaging data in 81 healthy subjects (Mori et al., 2008). This topography indicates for each voxel in imaging space a probability between 0 and 1 to belong to the CST. For 'CST load' (Zhu et al., 2010), the overlap between lesion map and the probabilistic CST map is weighted by a voxel's probability to be part of the CST. Accordingly, lesioned voxel that are more likely to be part of the CST contribute more to the CST lesion metric. For 'weighted CST load' (Zhu et al., 2010), the overlap between lesion map and the probabilistic CST map is weighted by the probability of a voxel to be part of the CST, and each voxel's contribution is weighted by the cross-sectional area of the CST on each axial slice of the brain atlas. Accordingly, lesioned voxel in dense parts of the CST fibre bundle contribute more to the CST lesion metric. Computations were performed in MATLAB 2019b using SPM 12 algorithms. For more details on CST lesion metrics, see the formulas in Zhu et al. (2010) and the current study's documented scripts, as available in the online materials. Final results for both CST biomarkers were highly similar, and thus results for weighted CST load are reported in the supplementary.

To ensure that topographical signal strength, as assessed by maximum Z values in the univariate lesion behaviour mapping analysis, is comparable between upper limb paresis (acute paresis max Z = 6.77; chronic paresis max Z = 6.58) and CST load (max Z = 8.25), random noise was added similar as in recent studies (Pustina et al., 2018). Noisy CST biomarkers were created by choosing a noise factor n in the range $0 < n < 1$ and calculating noisy biomarkers $nCST_{bm}$ based on original

biomarkers CST_{bm} and uniform random values between 0 and 1 by $nCST_{bm} = n * CST_{bm} + (1-n) * rand[0:1] * \max(CST_{bm})$. Factor n was tested in steps of 0.05 and manually chosen to provide optimal comparability between analyses of upper limb paresis and CST lesion biomarkers. For more information, see the online materials of the present study. The maximum Z value for noisy CST load (max Z = 6.92) was comparable in signal strength to upper limb paresis. Note that both original and noisy CST lesion biomarkers were mapped and interpreted.

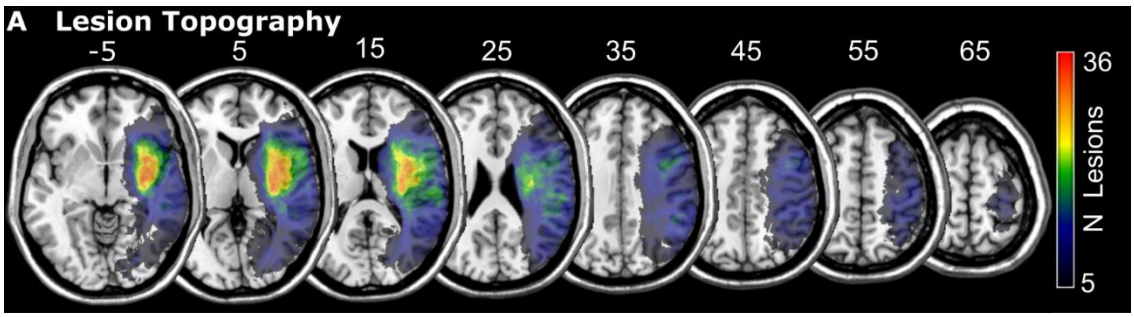

Figure 1: Lesion topography

Overlap topography of all 102 normalized binary lesion maps. The total number of overlapping lesions per voxel is depicted. Only voxel damaged in at least 5 patients are shown, which corresponds to the voxel included in the analyses. Numbers above the slices indicate z-coordinates in MNI space.

Lesion behaviour mapping

The relation between voxel-wise lesion status and motor variables was mapped by univariate voxel-based lesion behaviour mapping (VLBM) and multivariate lesion behaviour mapping (MLBM). All analyses were conducted at p = 0.05 only including voxel affected in at least five patients. VLBM was performed with voxel-wise general linear models, in the current study equivalent to t-tests, to investigate the relation between a voxel's binary lesion status and the behavioural target variable in NiiStat (https://www.nitrc.org/projects/niistat/). Family-wise error correction for multiple comparisons was applied by maximum statistic permutation thresholding with 1,000 permutations. MLBM was performed with support vector regression-based lesion symptom mapping (SVR-LSM; Zhang et al., 2014). Contrary to the typical procedures chosen in previous brain mapping studies using SVR-LSM (Zhang et al., 2014; Sperber et al., 2019), the present study aimed at a high comparability with

prediction studies that directly utilized voxel-wise lesion data to predict the target variable (e.g. Rondina et al., 2016; Hope et al., 2018). Therefore, contrary to procedures common to mapping the functional architecture of the brain (Zhang et al., 2014; DeMarco & Turkeltaub, 2018; Sperber et al., 2019), lesion data were not controlled for lesion size, and a support vector regression with linear kernel and hyperparameter $C = 2^{-16}$, which was found to be optimal for structural lesion data by hyperparameter optimization in a previous study (Sperber, 2020), was used in libSVM (Chang & Lin, 2011). This allowed investigating which areas in the brain provide information that is utilized by a high-dimensional algorithm to model hemiparesis. Topographies controlled for lesion size are included in the online material. The contribution of each voxel's data to the model was assessed by computing the linear feature weights. Topographical inference was carried out by a permutation approach which re-computed the support vector regression with the same imaging data and permuted behavioural data 5000 times. Voxel-wise statistical significance was then assigned by comparison of the true feature weights with the permutation-derived feature weights. The resulting statistical topography was corrected by false discovery rate (FDR, Bejamini & Yekutieli, 2001) at $q = 0.05$. Largest clusters in the topographical statistical results were assigned to brain regions by reference to the AAL atlas and a selection of fibre tracts found in the JHU white matter atlas in mricron (https://www.nitrc.org/projects/mricron), and the probabilistic map of the CST (Mori et al., 2008). For detailed descriptive data and underlying topographies, see the online materials.

Data availability

Online materials including all analysis scripts, descriptive data, and resulting topographies are publicly available at http://dx.doi.org/10.17632/2pj8nxwbxr.1. The clinical datasets analysed in the current study are not publicly available due to the data protection agreement approved by the local ethics committee and signed by the participants. They are available from Hans-Otto Karnath (karnath@uni-tuebingen.de) on reasonable request.

Results

Neural correlates of upper limb paresis

Mapping the neural correlates of acute upper limb paresis with VLBM (Figure 2A)

found significant voxel centred on the CST, but also extending beyond the CST into insula, putamen, rolandic (fronto-parietal) operculum, postcentral gyrus, superior temporal gyrus, hippocampus, external capsule, corona radiata, and superior longitudinal fasciculus. The results for MLBM (Figure 2B) even extended much further into many areas of the middle cerebral artery territory including frontal, temporal, and parietal areas. Note that larger clusters were expected here, as MLBM was not controlled for lesion size and, contrary to VLBM, corrected by more liberal FDR correction.

Mapping chronic upper limb paresis with VLBM (Figure 2C), no significant results were located in the CST. Instead, small clusters were found located in post- and precentral gyrus, and rolandic operculum. Using MLBM (Figure 2D), results included the CST, and further pre- and postcentral gyri, inferior and middle frontal gyrus, rolandic operculum, hippocampus, caudatum, putamen, pallidum, superior temporal gyrus, and external capsule.

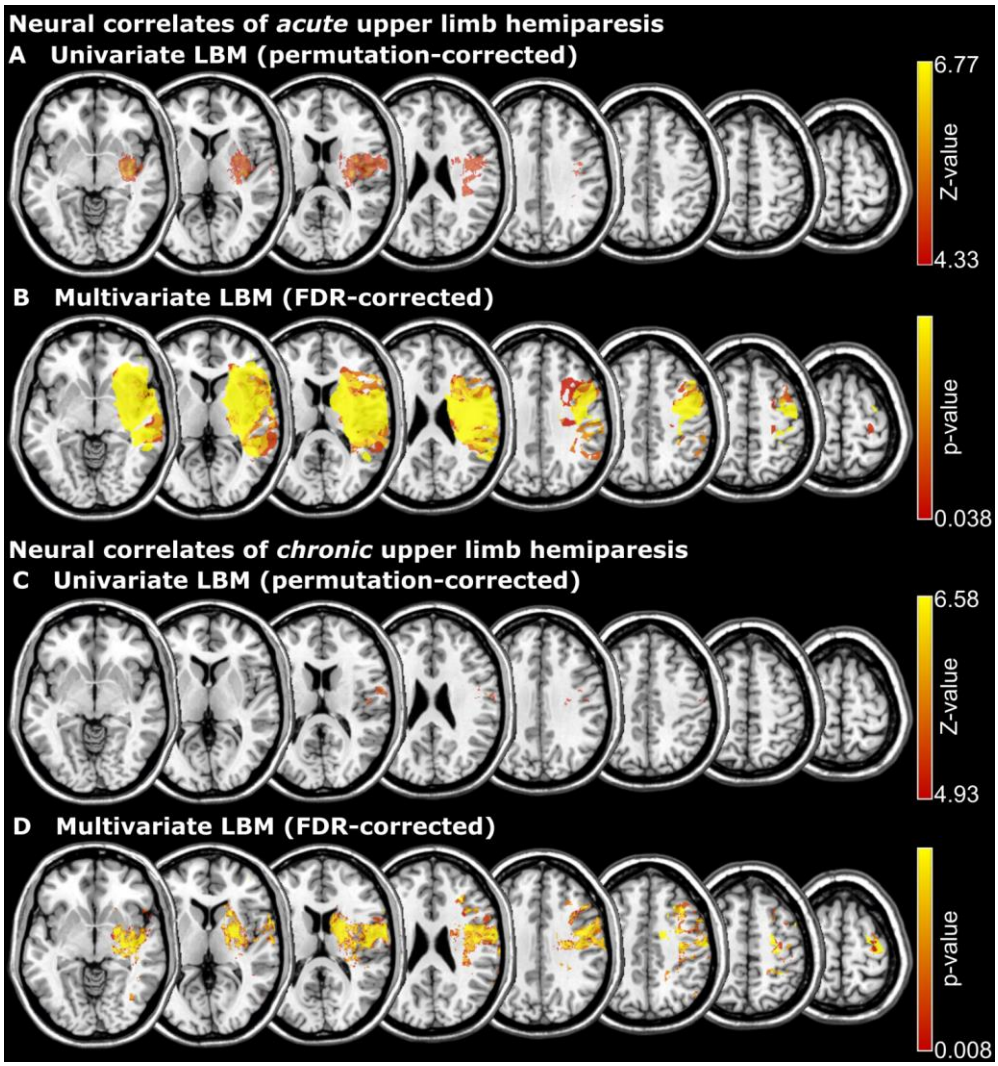

Figure 2: Lesion mapping of upper limb paresis

Voxel-wise lesion behaviour mapping of upper limb paresis both for A) + B) acute and C) + D) chronic motor assessment. Note that, in the current study, multivariate lesion behaviour mapping was intentionally not utilized following current standard procedures for human brain mapping, and therefore univariate and multivariate methods cannot be directly compared.

Neural correlates of CST lesion biomarkers

Mapping the neural correlates of 'CST load' without noise using VLBM (Figure 3A) found significant cluster in the CST, but also extending into pre- and post-central gyri, inferior, middle, and superior frontal gyri, supramarginal gyrus, rolandic operculum, superior temporal gyrus, putamen, pallidum, thalamus, superior longitudinal fasciculus, and corona radiata. For MLBM of 'CST load' without noise (Figure 3B), also features in the CST were significant, and additionally features in pre- and post-central gyri, middle frontal gyrus, supramarginal gyrus, rolandic operculum, superior temporal gyrus, putamen, pallidum, caudatum, thalamus, superior longitudinal fasciculus, and corona radiata.

Mapping the neural correlates of CST load with noise found, as expected, less significant voxel, due to reduced signal. Using VLBM (Figure 3C), significant voxel were found in pre- and postcentral gyrus, rolandic operculum, putamen, supramarginal gyrus, external capsule, corona radiata, and superior longitudinal fascicle. Using MLBM (Figure 3D), CST lesion load with noise was associated with damage in pre- and postcentral gyrus, rolandic operculum, putamen, pallidum, superior temporal gyrus, caudatum, hippocampus, supramarginal gyrus, thalamus, external capsule, corona radiata, and superior longitudinal fascicle.

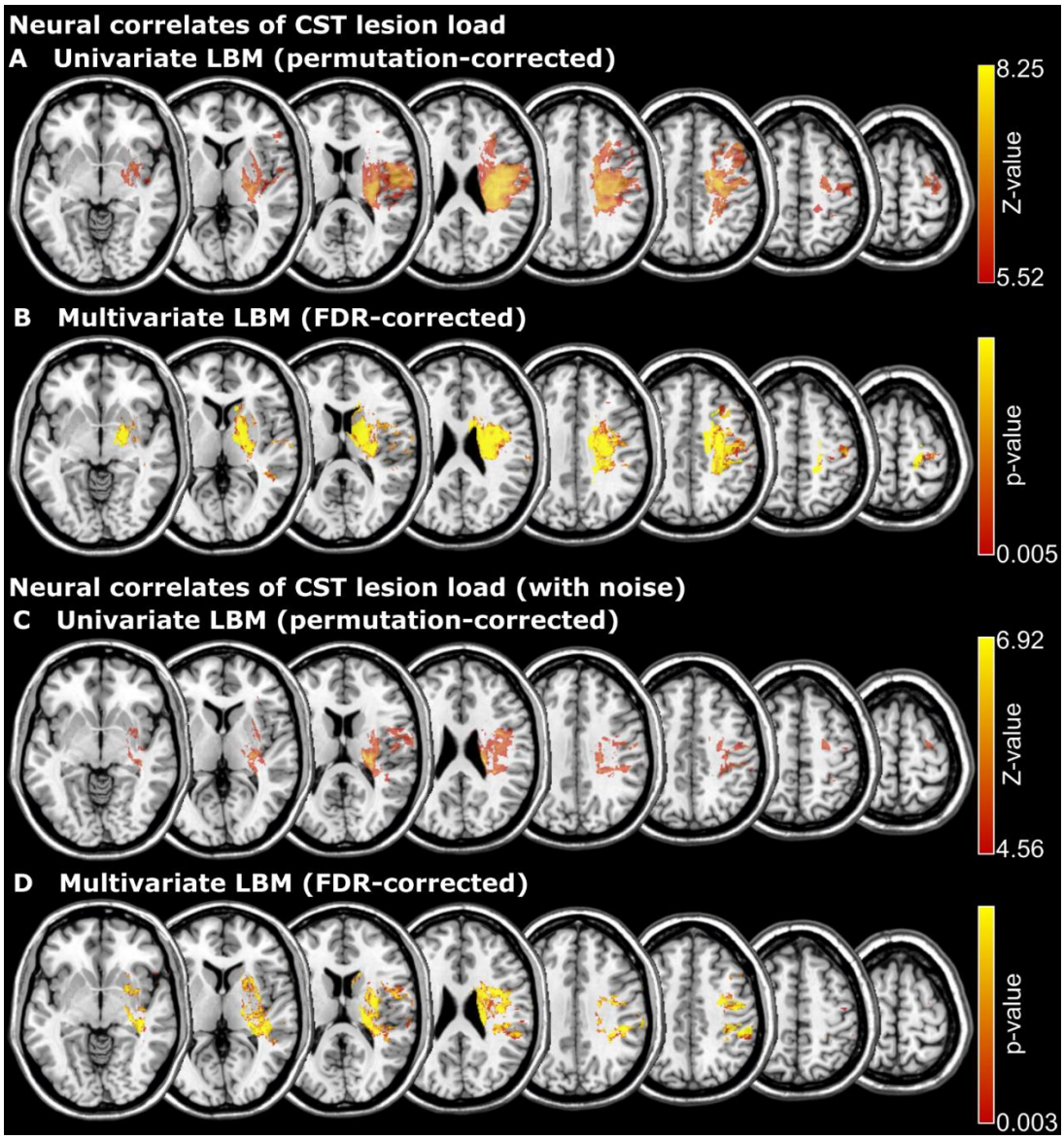

Figure 3: Lesion mapping of CST load

Voxel-wise lesion behaviour mapping of CST load both for A) + B) raw lesion load scores and C) + D) lesion load scores with noise added to match peak statistical signal with the mapping of upper limb paresis scores.

Results for weighted CST load (supplementary Figure 1) closely resembled results for CST load and were thus not consulted in the data interpretation process. Topographies can be found in the supplementary and in the online materials of the present study.

Next, topographies of upper limb paresis and CST lesion biomarkers were directly compared. First, univariate VLBM topographies of acute upper limb paresis and CST load with noise were contrasted (Figure 4A). This comparison was chosen as it mirrors a typical design to map the human brain (Karnath & Rennig, 2017), where

univariate statistics are commonly applied on acute stroke data. Several areas outside the CST were found to be associated with both variables, including rolandic operculum, putamen, external capsule, superior longitudinal fascicle, and corona radiata. Second, multivariate LBM topographies were compared between chronic upper limb paresis and CST load with noise (Figure 4B). This comparison was chosen as it corresponds to a typical design in post stroke outcome prediction, where multivariate models are used to predict chronic outcome (e.g. Hope et al., 2018; Nachev et al., 2019). In the current study, multivariate LBM identified voxel with a potential informative value in long-term outcome prediction. Again, several areas outside the CST were found to be associated with both variables, including rolandic operculum, putamen, pre- and postcentral gyri, hippocampus, external capsule, superior longitudinal fascicle, and corona radiata.

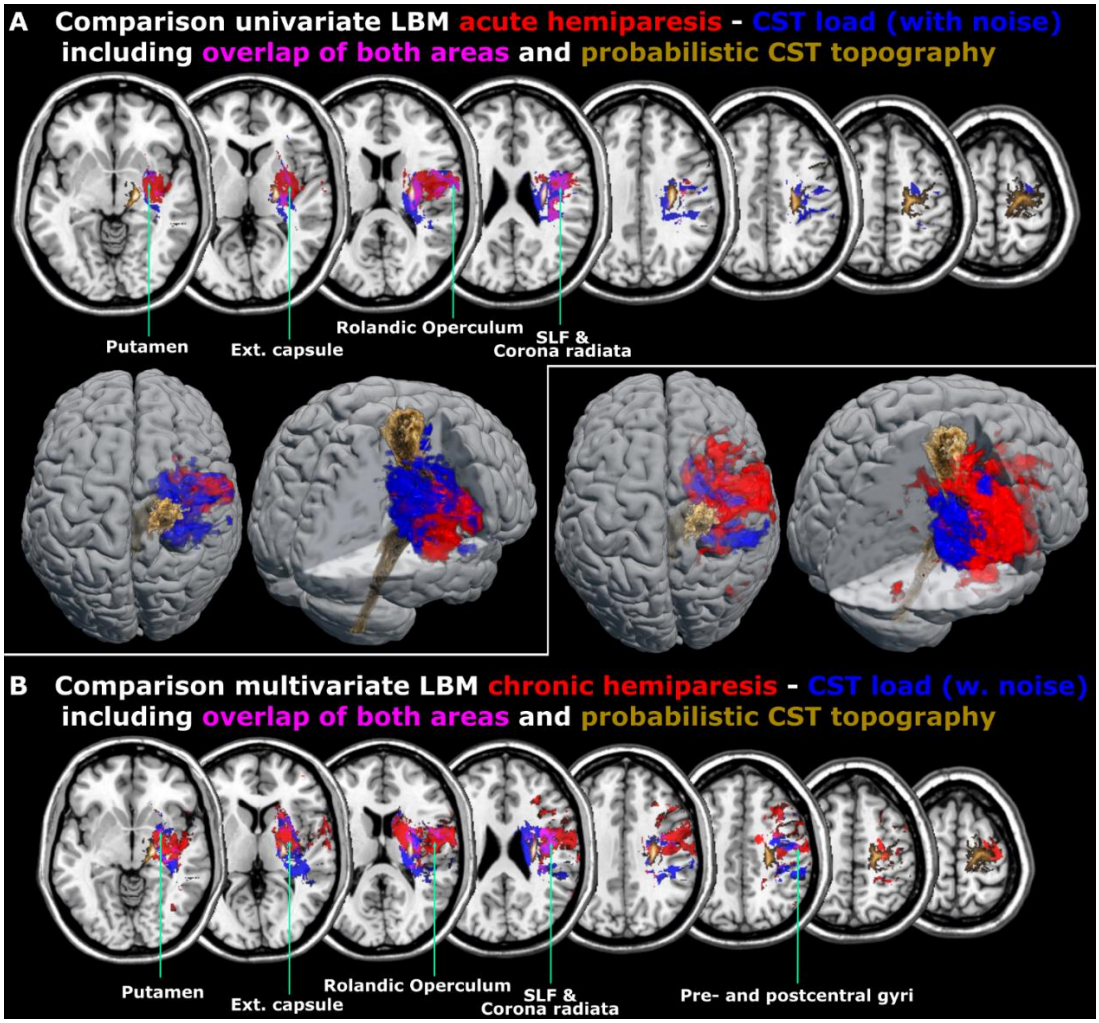

Figure 4: Comparison of the neural correlates of upper limb paresis and CST load

Direct comparison of statistical topographies in relation to the probabilistic topography of the CST. A) Comparison of univariate VLBM between acute upper limb paresis and CST load (with noise). B) Comparison of MLBM between chronic upper limb paresis and CST load (with noise). Areas of overlap are indicated and labelled. SLF = superior longitudinal fascicle

Discussion

We mapped the neural correlates of upper limb paresis and of CST lesion biomarkers. The latter, per definition, only represent damage to the CST. In all mapping analyses of acute or chronic upper limb paresis, areas outside of the primary motor system were revealed. This could suggest that upper limb paresis is not only caused by damage to the primary motor system, but also by damage to additional brain areas. However, mapping CST lesion biomarkers also implicated several areas outside of the CST, with some correspondence to the areas implicated in upper limb paresis. Lesion information from these areas also significantly contributed to high-dimensional models for long-term motor outcome. Damage to these areas might not play a causal role in hemiparesis, while still providing predictive value for post-stroke motor outcome. These findings impose the need to rethink feature selection strategies in post-stroke outcome prediction based on imaging data.

At first, it might appear counter-intuitive that CST lesion biomarkers are related to damage to areas outside of the CST. This finding is based on the systematic complexity of brain lesions. Stroke follows the vasculature, resulting in typical stroke patterns, and neighbouring brain regions are systematically damaged together. Thus, even if upper limb paresis was caused only by damage to primary motor regions, mapping hemiparesis would implicate areas outside of the primary motor system. This caveat of all current lesion-deficit inference methods has been acknowledged recently (Mah et al., 2014; Sperber et al., 2019; Sperber 2020). Notably, these areas outside of the primary motor system are predictive of hemiparesis, even if they are not directly causally related. In general, predictions can be made based on variables that are not the direct cause of the target variable: we can predict the weather from a swallow's flight, even though it is not the swallow that causes rain. The general need to differentiate between direct causality and predictive value in feature selection of imaging biomarkers is illustrated with a fictional example in Figure 5.

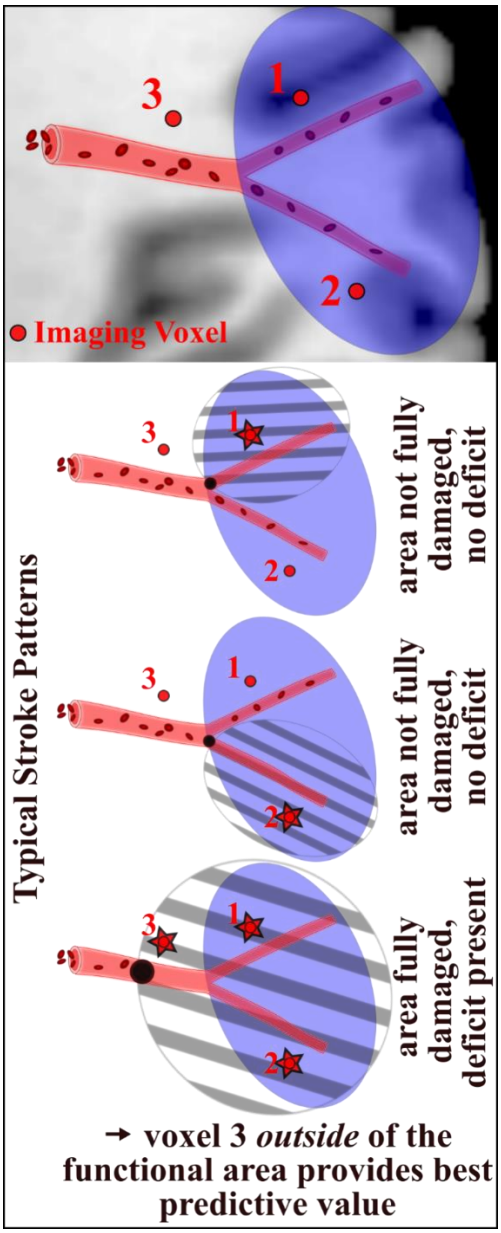

Figure 5: A fictional example to illustrate the discrepancy between functional brain anatomy and predictive value in stroke imaging biomarkers

The neural correlates of a behaviour (blue area) is supplied by two branches of an artery. Only full damage to the area evokes a deficit. Given the typical anatomy of lesions – after ischemia in either of the branches, or the preceding artery – imaging information taken from inside the neural correlates (voxel 1 & 2) provide only sub-optimally predictive value for the deficit. On the other hand, information taken from outside the neural correlate (voxel 3) might even surpass the predictive value of single imaging features obtained from the area where damage actually caused the symptom.

Several previous studies suggested that features taken from regions outside of the primary motor system should be included in post-stroke outcome prediction (Park et al., 2016; Rondina et al., 2016; Rondina et al., 2017). The rationale behind this approach was theories that causally link these regions and primary motor deficits, e.g. the assumption that these areas are relevant for motor and sensory function (Rondina et al., 2016; Rondina et al., 2017). Indeed, prediction performance was improved by this strategy, but the present study suggests that this might have happened for other reasons. Some of the proposed motor regions overlapped with regions that were found to be associated with CST biomarkers in the present study, including subcortical and frontal regions. Notably, several of the proposed motor areas were not found to be

related to motor deficits in the present study, and thus likely only a subset of regions underlay the improvement in prediction. The question remains which areas outside of the primary motor system actually play a direct causal role in primary motor deficits, and if this was the case for at least some of the regions chosen by previous prediction studies. The current study was not designed to identify what areas constitute the true neural correlates of upper limb paresis. Our findings rather imply that topographical results have to be interpreted with caution, and favour the view that the combination of lesion-deficit inference with strong hypotheses and behavioural experiments (Rinne et al., 2017), or other imaging and neurostimulation techniques is required to provide a solid foundation to understand the architecture of the human motor system and the human brain in general (Rorden & Karnath, 2004).

Conclusions

Post-stroke outcome prediction based on clinical imaging has potential to revolutionize individual patient care. Clinical imaging is part of any diagnostic protocol, and algorithms using only such data would be widely applicable and economic. However, no effective algorithms exist yet (Nachev et al., 2019). Low-dimensional prediction algorithms, such as simple linear regression, achieve up to moderate prediction performance at best based on CST lesion biomarkers (Findlater et al., 2019). For clinically useful algorithms, prediction performance has to be further improved, and high-dimensional models will likely be required to achieve this (Nachev et al., 2019). Feature selection is a vital step in any such algorithm based on machine learning. The current study indicates that this is a difficult task in stroke imaging data, which are highly complex and inter-related. Choosing features based on our understanding of the brain might perform sub-optimally, even for – compared to the complex language or spatial attention systems – relatively well-understood and more easily accessible brain functions such as primary motor abilities. Instead, data-driven feature selection strategies might be required to improve prediction algorithms and bring us closer to effective predictive personalized medicine.

Declaration of Conflicting Interests

The authors declare that there is no conflict of interest.

Funding

This work was supported by the German Research Foundation (KA 1258/23-1).

References

Buch ER, Rizk S, Nicolo P, Cohen LG, Schnider A, Guggisberg AG (2016): Predicting motor improvement after stroke with clinical assessment and diffusion tensor imaging. Neurology 86:1924–5. http://www.ncbi.nlm.nih.gov/pubmed/27164664.

Chang C, Lin C (2011): LIBSVM: A Library for Support Vector Machines. ACM Trans Intell Syst Technol 2:1–27. https://dl.acm.org/doi/10.1145/1961189.1961199.

DeMarco AT, Turkeltaub PE (2018): A multivariate lesion symptom mapping toolbox and examination of lesion-volume biases and correction methods in lesion-symptom mapping. Hum Brain Mapp 39:4169–4182. http://doi.wiley.com/10.1002/hbm.24289.

Feng W, Wang J, Chhatbar PY, Doughty C, Landsittel D, Lioutas V-A, Kautz S, Schlaug G (2015): Corticospinal tract lesion load - A potential imaging biomarker for stroke motor outcomes. Ann Neurol. http://www.ncbi.nlm.nih.gov/pubmed/26289123.

Findlater SE, Hawe RL, Mazerolle EL, Al Sultan AS, Cassidy JM, Scott SH, Pike GB, Dukelow SP (2019): Comparing CST Lesion Metrics as Biomarkers for Recovery of Motor and Proprioceptive Impairments After Stroke. Neurorehabil Neural Repair 33:848–861.

Frenkel-Toledo S, Fridberg G, Ofir S, Bartur G, Lowenthal-Raz J, Granot O, Handelzalts S, Soroker N (2019): Lesion location impact on functional recovery of the hemiparetic upper limb. Ed. Mariella Pazzaglia. PLoS One 14:e0219738. http://dx.plos.org/10.1371/journal.pone.0219738.

Hope TMH, Leff AP, Price CJ (2018): Predicting language outcomes after stroke: Is structural disconnection a useful predictor? NeuroImage Clin 19:22–29. https://linkinghub.elsevier.com/retrieve/pii/S2213158218301074.

Karnath H-O, Rennig J (2017): Investigating structure and function in the healthy human brain: validity of acute versus chronic lesion-symptom mapping. Brain Struct Funct 222:2059–2070. http://link.springer.com/10.1007/s00429-016-1325-7.

Lindenberg R, Renga V, Zhu LL, Betzler F, Alsop D, Schlaug G (2010): Structural integrity of corticospinal motor fibers predicts motor impairment in chronic stroke. Neurology 74:280–287. http://www.pubmedcentral.nih.gov/articlerender.fcgi?artid=3122304&tool=pmcentrez&rendertype=abstract.

Lo R, Gitelman D, Levy R, Hulvershorn J, Parrish T (2010): Identification of critical areas for motor function recovery in chronic stroke subjects using voxel-based lesion symptom mapping. Neuroimage 49:9–18. http://linkinghub.elsevier.com/retrieve/pii/S1053811909009549.

Mah Y-H, Husain M, Rees G, Nachev P (2014): Human brain lesion-deficit inference remapped. Brain 137:2522–31. http://www.ncbi.nlm.nih.gov/pubmed/24974384.

Mori S, Oishi K, Jiang H, Jiang L, Li X, Akhter K, Hua K, Faria A V., Mahmood A, Woods R, Toga AW, Pike GB, Neto PR, Evans A, Zhang J, Huang H, Miller MI, van Zijl P, Mazziotta J (2008): Stereotaxic white matter atlas based on diffusion tensor imaging in an ICBM template. Neuroimage 40:570–582. http://www.ncbi.nlm.nih.gov/pubmed/18255316.

Nachev P, Rees G, Frackowiak R (2018): Lost in translation. F1000Research 7:620. https://www.scopus.com/inward/record.uri?eid=2-s2.0-84956939146&doi=10.1056%2FNEJMp1511412&partnerID=40&md5=a2a39037de1b7900de2ef54ace04b0b2.

Park CH, Kou N, Ward NS (2016): The contribution of lesion location to upper limb deficit after stroke. J Neurol Neurosurg Psychiatry 87:1283–1286.

Pustina D, Avants B, Faseyitan OK, Medaglia JD, Coslett HB (2018): Improved accuracy of lesion to symptom mapping with multivariate sparse canonical correlations. Neuropsychologia 115:154–166. http://dx.doi.org/10.1016/j.neuropsychologia.2017.08.027.

Rinne P, Hassan M, Fernandes C, Han E, Hennessy E, Waldman A, Sharma P, Soto D, Leech R, Malhotra PA, Bentley P (2017): Motor dexterity and strength depend upon integrity of the attention-control system. Proc Natl Acad Sci:201715617. http://www.pnas.org/lookup/doi/10.1073/pnas.1715617115.

Rondina JM, Filippone M, Girolami M, Ward NS (2016): Decoding post-stroke motor function from structural brain imaging. NeuroImage Clin 12:372–380. http://dx.doi.org/10.1016/j.nicl.2016.07.014.

Rondina JM, Park C, Ward NS (2017): Brain regions important for recovery after severe post-stroke upper limb paresis. J Neurol Neurosurg Psychiatry 88:737–743. http://jnnp.bmj.com/lookup/doi/10.1136/jnnp-2016-315030.

Rorden C, Karnath HO (2004): Using human brain lesions to infer function: A relic from a past era in the fMRI age? Nat Rev Neurosci 5:812–819. http://www.ncbi.nlm.nih.gov/pubmed/15378041.

Rorden C, Bonilha L, Fridriksson J, Bender B, Karnath HO (2012): Age-specific CT and MRI templates for spatial normalization. Neuroimage 61:957–965. http://www.ncbi.nlm.nih.gov/pubmed/22440645.

Sperber C (2020): Rethinking causality and data complexity in brain lesion-behaviour inference and its implications for lesion-behaviour modelling. Cortex 126:49–62. https://doi.org/10.1016/j.cortex.2020.01.004.

Sperber C, Wiesen D, Karnath HO (2019): An empirical evaluation of multivariate lesion behaviour mapping using support vector regression. Hum Brain Mapp 40:1381–1390. https://onlinelibrary.wiley.com/doi/abs/10.1002/hbm.24476.

Sterr A, Dean PJ a., Szameitat AJ, Conforto AB, Shen S (2014): Corticospinal Tract Integrity and Lesion Volume Play Different Roles in Chronic Hemiparesis and Its Improvement Through Motor Practice. Neurorehabil Neural Repair 28:335–343. http://nnr.sagepub.com/cgi/doi/10.1177/1545968313510972.

Stinear CM, Barber PA, Petoe M, Anwar S, Byblow WD (2012): The PREP algorithm predicts potential for upper limb recovery after stroke. Brain 135:2527–2535.

Wang LE, Tittgemeyer M, Imperati D, Diekhoff S, Ameli M, Fink GR, Grefkes C (2012): Degeneration of corpus callosum and recovery of motor function after stroke: A multimodal magnetic resonance imaging study. Hum Brain Mapp 33:2941–2956. http://doi.wiley.com/10.1002/hbm.21417.

Wenzelburger R (2005): Hand coordination following capsular stroke. Brain 128:64–74. https://academic.oup.com/brain/article-lookup/doi/10.1093/brain/awh317.

Yekutieli D, Benjamini Y (2001): The control of the false discovery rate in multiple testing under dependency. Ann Stat 29:1165–1188. http://www.ncbi.nlm.nih.gov/pubmed/18298808.

Zhang Y, Kimberg DY, Coslett HB, Schwartz MF, Wang Z (2014): Multivariate lesion-symptom mapping using support vector regression. Hum Brain Mapp 35:5861–5876.

Zhu LL, Lindenberg R, Alexander MP, Schlaug G (2010): Lesion load of the corticospinal tract predicts motor impairment in chronic stroke. Stroke 41:910–5. http://www.ncbi.nlm.nih.gov/pubmed/20378864.